GeoHealth

RESEARCH ARTICLE

10.1029/2024GH001290

$PM_{2.5}$-Associated Premature Mortality Attributable to Hot-And-Polluted Episodes and the Inequality Between the Global North and the Global South

Tao Huang[1,2], Yue Li[2], Jinhui Li[3], Joseph J. Y. Sung[1], and Steve H. L. Yim[1,2,4,5]

[1]Lee Kong Chian School of Medicine, Nanyang Technological University, Singapore, Singapore, [2]Centre for Climate Change and Environmental Health, Nanyang Technological University, Singapore, Singapore, [3]Department of Urology, Stanford University Medical Center, Stanford, CA, USA, [4]Earth Observatory of Singapore, Nanyang Technological University, Singapore, Singapore, [5]Asian School of the Environment, Nanyang Technological University, Singapore, Singapore

Abstract Exposure to air pollution and excessive heat during hot-and-polluted episodes (HPEs) may synergistically cause higher health risks globally. Nevertheless, long-term global spatiotemporal characteristics of HPEs and their health impacts remain unclear. Herein, we conducted statistical analyses using reanalysis data of fine particulate matter ($PM_{2.5}$) and climate together with our derived concentration-response function for HPEs to assess global HPE variations from 1990 to 2019, and to estimate the $PM_{2.5}$-associated premature mortality during HPEs. Our results reveal that HPE frequency increased significantly globally. HPE $PM_{2.5}$ intensity in the Global North continuously increased, overpassing the Global South after 2010, indicating a recurred risk of air pollution under climate change in the Global North after several years of emission control endeavors. Globally, we estimated approximately 694,440 (95% CI: 687,996–715,311) total mortalities associated with acute $PM_{2.5}$ exposure during HPEs from 1990 to 2019, with the Global South accounting for around 80% of these deaths. Among the most vulnerable 15 countries, India had by far the highest mortality burden, and the United States, Russia, Japan, and Germany were particularly highlighted as having higher burdens within the Global North. Our findings highlight the importance of considering environmental inequality between the Global North and the Global South, and co-benefits of air pollution-climate change mitigation during policymaking processes.

Plain Language Summary Exposure to air pollution and heat during hot-and-polluted episodes (HPEs) can combine to increase health risks worldwide. However, we still do not fully understand the long-term global patterns of HPEs or their health effects. This study analyzed global data on air pollution ($PM_{2.5}$) and climate from 1990 to 2019 to understand how HPEs have changed over time. We also estimated the number of premature deaths linked to $PM_{2.5}$ during HPEs using the concentration-response function we developed. Results show HPEs have become more frequent across the world. In the Global North, $PM_{2.5}$ levels during HPEs have steadily increased, surpassing levels in the Global South after 2010. This trend suggests a return of $PM_{2.5}$ risks in the Global North despite years of efforts to reduce emissions. We estimated that $PM_{2.5}$ during HPEs caused about 694,440 premature deaths globally between 1990 and 2019. Around 80% of these deaths occurred in the Global South, highlighting unequal health burdens. Among the most affected countries, India had the highest number of deaths, while the U.S., Russia, Japan, and Germany stood out in the Global North. These results emphasize the need to address global environmental inequality and to combine efforts to tackle both air pollution and climate change.

Key Points:

- HPE frequency and $PM_{2.5}$ intensity during HPEs have increased globally, with the Global North surpassing the Global South after 2010
- Acute $PM_{2.5}$ exposure during HPEs caused around 694,440 premature deaths globally from 1990 to 2019, with 80% occurring in the Global South
- Environmental inequality highlights the need to integrate air pollution and climate change mitigation in policymaking

Supporting Information:

Supporting Information may be found in the online version of this article.

Correspondence to:

S. H. L. Yim,
yimsteve@gmail.com

Citation:

Huang, T., Li, Y., Li, J., Sung, J. J. Y., & Yim, S. H. L. (2025). $PM_{2.5}$-associated premature mortality attributable to hot-and-polluted episodes and the inequality between the Global North and the Global South. *GeoHealth*, *9*, e2024GH001290. https://doi.org/10.1029/2024GH001290

Received 25 NOV 2024
Accepted 20 MAR 2025

Author Contributions:

Conceptualization: Steve H. L. Yim
Formal analysis: Tao Huang, Yue Li, Jinhui Li, Joseph J. Y. Sung, Steve H. L. Yim
Funding acquisition: Steve H. L. Yim
Investigation: Steve H. L. Yim
Methodology: Tao Huang
Project administration: Steve H. L. Yim
Software: Tao Huang
Supervision: Steve H. L. Yim
Validation: Tao Huang
Visualization: Tao Huang

1. Introduction

Air pollution and extreme heat are two fatal factors to adverse public health outcomes (Gu & Yim, 2016; Hong et al., 2019; Y. Xu et al., 2013; Zhang et al., 2009). Epidemiological studies have reported that ambient air pollution, particularly particulate matter with a diameter of 2.5 μm or less ($PM_{2.5}$), substantially impacts human health, causing an estimated 4.5 million deaths worldwide in 2015 (A. J. Cohen, Brauer, et al., 2017; Pozzer et al., 2023). Exposure to $PM_{2.5}$ has been reported to induce risks in acute diseases, including both respiratory and cardiovascular diseases (Janssen et al., 2013; T. Li et al., 2019; Wei, Li, et al., 2023). The adverse impacts also extend to cognitive functions, affecting both the mental and physical aspects of the brain (Hansen et al., 2008; Thompson et al., 2023; Underwood, 2017). Moreover, the frequency of heatwaves has been reported to increase in

Writing – original draft: Tao Huang
Writing – review & editing: Yue Li, Jinhui Li, Joseph J. Y. Sung, Steve H. L. Yim

recent years (Dong et al., 2021; McKinnon & Simpson, 2022), and this has also been recognized as a potentially fatal factor affecting human health (Borchers Arriagada et al., 2020; Campbell et al., 2018; Chambers, 2020). The co-occurrence of air pollution and heatwave in an episode [hot-and-polluted episode (HPE)] (Nduka et al., 2022; Yim, 2020) may also become increasingly prevalent with the growing population and global warming (Anenberg et al., 2020). High temperature may further enhance the adverse health impact of exposure to $PM_{2.5}$ (Nduka et al., 2022). Recent research has reported possible mechanisms through which heat exacerbates illnesses induced by air pollution (Parliari et al., 2024). The findings of these studies showed that increased inflammation is susceptible to thermoregulation of the human body (McGeehin & Mirabelli, 2001), while inflammation plays a crucial role in both the pathogenesis and exacerbation of illnesses, such as asthma and chronic obstructive pulmonary disease, and inflammation can be triggered by exposure to air pollutants. Also, high ambient temperature and air pollution could both accelerate DNA methylation (Chiu et al., 2024; Mukherjee et al., 2021), which is associated with poor respiratory health outcomes (Rider & Carlsten, 2019). Given the increasing concern regarding this joint impact of HPEs, the premature mortalities associated with acute exposure to $PM_{2.5}$ during HPE need to be assessed.

Very limited studies focused on the synergistic impacts of high temperature on $PM_{2.5}$ associated premature mortality when estimating the relative risk using concentration-response functions (CRFs). Typically, when deriving a CRF based on daily mortality rates and air pollution exposure, most of the published epidemiological studies regarded temperature as a confounder instead of a modifier in their models, trying to eliminate the impacts of ambient temperature on their estimate of $PM_{2.5}$-associated mortality (Atkinson et al., 2014; Moolgavkar, 2003; Vanos et al., 2015). Recently, with the co-occurrence of air pollution and heatwaves being recognized as a deadly combination (Kinney & Pinkerton, 2022), the synergistic effect of high environmental temperature needs to be taken into account in the process of deriving CRFs. Moreover, local scale studies, which are typically conducted within specific cities, countries, or regions, limit their broader applicability worldwide. For instance, the predominant focus on urban regions within Europe (Doherty et al., 2017; Janssen et al., 2013; Pascal et al., 2014), North America (Curriero et al., 2002; Deschênes & Greenstone, 2011), and China (Gu & Yim, 2016; Health, 2023; Hong et al., 2019) does not facilitate equitable comparisons of health burdens across diverse global regions, thereby hindering a comprehensive understanding of the worldwide situation (Liu et al., 2019). Also, ozone (Y. Xu et al., 2020) was more investigated than $PM_{2.5}$ in prior studies due to its correlation with high temperature, but there are few long-term assessments spanning decades. These highlight the need for a comprehensive understanding of global HPE evolution during past decades, and for deriving a CRF to estimate the global burden of mortality associated with $PM_{2.5}$ exposure under the synergistic effect of heat during HPEs.

This study aimed to comprehensively analyze the global spatial and temporal characteristics of HPEs from 1990 to 2019 and to estimate the global premature mortality associated with exposure to $PM_{2.5}$ during HPEs. The statistical analyses based on long-term reanalysis data of climate and $PM_{2.5}$ were applied to assess the frequency, duration, intensity, and trends of HPEs during 1990–2019 at multiple spatial scales (the Global North and the Global South, and countries), and the concentration-response function was further derived to estimate the resultant $PM_{2.5}$-associated premature mortality during HPEs.

2. Materials and Methods

2.1. Definition of Hot-And-Polluted Episodes (HPEs)

We defined a HPE as an episode with the co-occurrence of both high temperature and $PM_{2.5}$ pollution (Yim, 2020). We defined a polluted day as a day in which the daily average $PM_{2.5}$ surface mass concentration exceeded the 75th percentile of the recorded daily $PM_{2.5}$ from 1990 to 2019 in each grid of the $PM_{2.5}$ data set and reached at least 15 μg m^{-3}; this definition excludes regions with very low-threshold concentration according to the World Health Organization (WHO) short-term $PM_{2.5}$ guidelines (WHO global air quality guidelines, 2021). There are three common indicators used to define hot days: the relative threshold of daily maximum temperature (T_{max}), the absolute threshold of T_{max}, and the wet-bulb temperature (T_w). In this study, we used a relative threshold of T_{max} exceeding the 90th percentile of T_{max} from 1990 to 2019 in each grid to define hot days. The relative threshold definition was widely used in heatwave studies (Perkins-Kirkpatrick & Lewis, 2020) and was considered more suitable for global-scale studies including different regions than an absolute value. We also compared the results of HPE characteristics with those using absolute thresholds of $T_{max} > 33$°C (Yim et al., 2019; Zong et al., 2022) (Figure S1 in Supporting Information S1). The results show that the absolute

threshold inevitably underestimates the HPE increase at higher latitudes where long-term T_{max} are lower than the tropics and subtropics, thus may ignore the health burden in the Global North in the context of climate change. In addition, wet-bulb temperature $T_{w,}$ considering the impact of humidity, has been widely used to define hot days when a T_w was higher than 25°C (Y. Xu et al., 2020). As T_w incorporates the impact of humidity, this parameter can represent heat from the thermal comfort perspective. In this study, we calculated T_w following the formula in Y. Xu et al. (2020) (Text S1 in Supporting Information S1). We found that T_w definition of hot days does not perform well in areas at higher latitudes with low humidity (Figure S2 in Supporting Information S1). Herein, we applied the relative threshold definition in this study. It is recommended that local data can be used to identify local HPEs for better capturing the local conditions.

2.2. Characteristics of HPEs

The frequency of HPEs is defined as the number of HPE days in each year (days per year). The HPE duration is defined as the longest period of a consecutive HPE in a particular year. To date, there is no clear definition of HPE intensity in previous studies. In this study, we separated the intensity of HPEs into two parts: 1. HPE $PM_{2.5}$ intensity was defined as the maximum concentration among all HPEs in a grid within a specific year; 2. HPE temperature intensity was defined as the maximum temperature among all HPEs in a grid within a specific year. This concept takes into account the attributes of both temperature and concentration during HPEs.

2.3. $PM_{2.5}$ Data Set

Global surface $PM_{2.5}$ mass concentration data were derived from the Modern-Era Retrospective analysis for Research and Applications, Version 2 (MERRA-2). The hourly $PM_{2.5}$ components of surface mass concentrations provided by MERRA-2 include dust with a diameter of 2.5 μm or less, sea salt with a diameter of 2.5 μm or less, black carbon, organic carbon, and sulfate. The hourly $PM_{2.5}$ concentration from 1990 to 2019 was thus computed from the hourly species concentration according to Buchard et al. (2016):

$$PM_{2.5} = [DUST_{2.5}] + [SS_{2.5}] + [BC] + 1.4 \times [OC] + 1.375 \times [SO_4], \quad (1)$$

where the $DUST_{2.5}$, $SS_{2.5}$, BC, OC, and SO_4 data sets can be obtained from the hourly product of MERRA-2. Daily $PM_{2.5}$ records used in this study was calculated based on hourly scale data set. A 3-day moving window was applied to the daily $PM_{2.5}$ record.

2.4. MERRA-2 Data Set Evaluation

To assess the reliability of the MERRA-2 data set, we referred to studies that compared this data set with observational measurements. For example, Buchard et al. (2017) evaluated $PM_{2.5}$ surface mass concentration in the United States and found good agreement with observations. For East Asia, we referred to the data evaluation in C. Fang et al. (2020), who validated the MERRA-2 black carbon mass concentration with local measurements in continental Southeast Asia, China, and India, especially at two stations, that is, in Bangkok, Thailand (Sahu et al., 2011) and Honai, Vietnam (J. B. Cohen, Lecoeur, & Hui Loong Ng, 2017). Y. Xu et al. (2020) also used daily PM data from MERRA-2 to analyze heatwave and high-PM events in South Asia. We thus considered the data set to be reliable for PM.

2.5. Daily Maximum Temperature

The daily maximum temperature (T_{max}) used in this study was obtained from the Water and Global Change (WATCH) Forcing Data methodology applied to the ERA5 reanalysis data (WFDE5) through the Copernicus Climate Change Service (C3S), Climate Data Store (Copernicus Climate Change Service, 2020; Cucchi et al., 2020). The WFDE5 provides global hourly bias-corrected reconstructions of near-surface meteorological variables, such as the air temperature at 2 m above the surface of land with a spatial resolution of 0.5° × 0.5°. The quality of the hourly temperature product was previously validated by Cucchi et al. (2020).

2.6. Estimation of the Global-Scale Relative Risk of Exposure to $PM_{2.5}$ in HPEs

We conducted a systematic review and literature meta-analysis to generate a global-scale concentration–response function (CRF) to reflect the health impacts of $PM_{2.5}$ exposure during HPEs. Due to the data availability, we

restricted air pollutants to $PM_{2.5}$ and did not consider studies focusing on PM_{10} or ozone, whereas health output was strictly defined as all-cause mortality. We searched the PubMed, Scopus, and Web of Science databases with the search terms "$PM_{2.5}$," "high temperature," and "heatwaves" for exposures and "all-cause mortality" for the outcome. We reviewed studies published before 31 December 2023. To include as many samples as possible in our search, we did not consider sex, age group, or exposure lag of the studies. We screened for reference duplicates using Zotero Desktop. We excluded studies that only reported cause-specific mortality (e.g., "cardiovascular" or "respiratory"). We excluded studies without accessible full text. Detailed information can be found in the PRISMA diagram (Figure S3 in Supporting Information S1). Eventually, 9 papers (Table S1 in Supporting Information S1) met the criteria for the final estimation of the global-scale formula.

2.7. Global Burden of Mortality

After the selection of the literature, we fitted the daily all-cause premature mortality associated with exposure to ambient $PM_{2.5}$ concentration. We collected the relative risk and ambient $PM_{2.5}$ concentration from all these published papers and applied the function below, which describes the relative risk in each grid with a given $PM_{2.5}$ concentration, to estimate the three parameters, namely, α, β, and δ, in the function (Y. Li et al., 2023; Yim et al., 2024):

$$RR_k = 1 + \alpha \cdot \{1 - \exp[-\beta(X_k - X_0)^{\delta}]\}, \quad (2)$$

where RR_k refers to the relative risk of $PM_{2.5}$ exposure and k represents each grid in the data set. X_k is the daily surface $PM_{2.5}$ concentration in each grid from the MERRA-2 data set. X_0 is the baseline exposure, which is 7 μg m^{-3} in this study. After obtaining the RR_k, the global estimate of the mortality burden was derived at the country level:

$$E = \sum_k (RR_k - 1)/RR_k \cdot P_k \cdot f, \quad (3)$$

where E is the final daily all-cause mortality associated with $PM_{2.5}$ exposure during HPEs. P_k is the population in each grid. We obtained a population data set from WorldPop from 2000 to 2019, which has a spatial resolution of ~100 km. We thus interpolated the population to match the exact spatial resolution of $PM_{2.5}$ for the calculation. For pre-2000 population data, the detailed process can be found in Text S1 in Supporting Information S1. f refers to the annual all-cause mortality rate derived from the Global Burden of Disease (GBD) in each country. To derive the daily mortality rate, we assumed that the annual mortality rate was affected by the daily mortality rate evenly and then divided f by 365, following the method used to derive the daily mortality rate in a previous study (Xiao et al., 2022). The categories of the Global North and the Global South countries were derived from the World Population Review website. Annual averages of HPE frequency, duration, and intensity were computed as the mean across all grid points within each region (i.e., the Global North and the Global South) to capture the overall spatial patterns over time.

2.8. Monte-Carlo Estimation

We used the Monte-Carlo approach to investigate the uncertainty of human health results, which has been introduced in our previous studies (T. Huang et al., 2024). We assumed a triangular probability distribution and obtained 1,000 parameter estimations of α, β, and δ. Each estimated parameter was then regarded as an input into the estimation of premature mortalities. The ultimate range of uncertainty was expressed by the median value and 95% confidence interval (CI) of these 1,000 health impact results to take into account the uncertainties from the data set, the RR equation, and the paper selection during the literature review.

3. Results

3.1. Global Increases in HPEs During 1990–2019

To assess the global spatiotemporal characteristics of HPEs, we identified HPEs based on a daily scale near-surface temperature and $PM_{2.5}$ data sets from 1990 to 2019 (see Methods). Our findings reveal that HPE frequency (defined as the number of HPE days per year) increased globally (Figure 1a) at a rate of approximately 1.6 days per decade on a global basis (Figure S4 in Supporting Information S1). Specifically, the HPE frequency

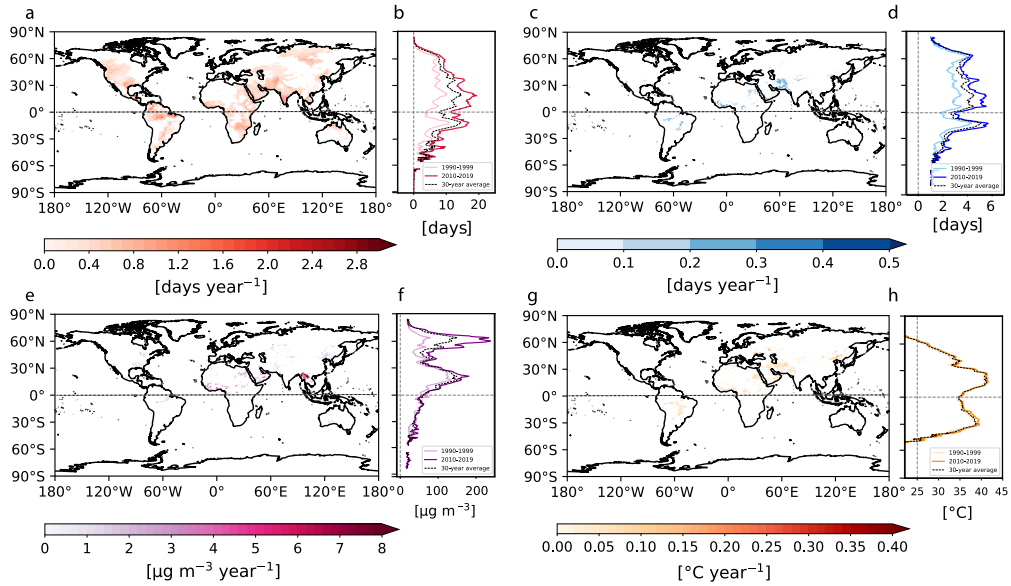

Figure 1. Global increases in Hot-and-Polluted Episode (HPE) frequency, duration, and intensity (including both $PM_{2.5}$ and temperature intensity) from 1990 to 2019. (a) Linear increase in annual HPE frequency from 1990 to 2019 in each grid ($0.5° \times 0.5°$). (b) Zonal-mean HPE frequency averaged in the first decade (1990–1999), the recent (2010–2019) decade, and the whole period (1990–2019). (c) Linear increase in annual HPE duration from 1990 to 2019 in each grid. (d) Same as (b) but for HPE duration (e) Linear increase in annual HPE $PM_{2.5}$ intensity from 1990 to 2019 in each grid. (f) Same as (b) and (d) but for HPE $PM_{2.5}$ intensity. (g) Linear increase in annual HPE temperature intensity from 1990 to 2019 in each grid. (h) Same as (b), (d), and (f) but for HPE temperature intensity. In (a), (c), (e), and (g), only results with significant linear increases ($r > 0$ and $p < 0.05$ in a linear regression t-test) are displayed. Figure (b), (d), and (f) share the same y-axis as (a), (c), (e), and (g), respectively.

increased from 4.2 days per year in the first decade (1990–1999) to 8.4 days per year in the recent decade (2010–2019) analyzed in this study. Regions with HPE frequency exceeding 15 days per year were mainly centralized in subtropical areas in both the Northern and Southern Hemispheres (Figure 1b). Substantial increases of more than 0.5 days per year were particularly pronounced in the Western and Southeastern parts of North America, the Caribbean, the Middle East, India, and continental Southeast Asia in the Northern Hemisphere (Figure 1a). In the Southern Hemisphere, similar increases were predominantly observed over the Amazon basin in South America, the southern part of Africa, and the northern part of Australia (Figure 1a). Notably, some regions that experienced rapid warming may not have exhibited a significant increase in HPEs due to insignificant changes in air pollution episodes, and vice versa. For example, despite a significant warming trend (Figure S5a in Supporting Information S1), maritime Southeast Asia experienced insignificant changes in air pollution episodes and, thus, an insignificant variation in HPE frequency (Figure S5b in Supporting Information S1). Our findings point out a significant increase in HPE frequency globally, particularly in the subtropical areas in both hemispheres from 1990 to 2019.

While the HPE frequency increased globally, significant variations in HPE duration [defined as the period (days) of the longest consecutive HPE in a particular year] occurred across only several regions: the coastal area along the Gulf of Mexico, the Amazon, West Africa, the Middle East, and continental Southeast Asia (Figure 1c). Maximum HPE duration longer than 5 days occurred within 30° latitude in the Southern Hemisphere (Figure 1d), attributed to prolonged HPE events in the Amazon area (Figure 1c). Another peak of around 4 days happened within approximately 30° in the Northern Hemisphere (Figure 1d). In these two peak regions, large-scale weather systems, such as the fluctuations in Rossby waves and atmospheric blocks, have been reported to induce prolonged heatwaves (D. Li et al., 2020; Qian et al., 2022).

The intensity of extreme climate events indicates the magnitude of hazards and may determine the severity of harm directly to human beings. To include impacts of both $PM_{2.5}$ pollution and heat, we separated the intensity of HPEs into two parts: the intensity of $PM_{2.5}$ (defined as the maximum $PM_{2.5}$ concentration among all HPEs within a specific year; see Methods) and the intensity of temperature (defined as the maximum temperature among all

HPEs within a specific year; see Methods). Regions exhibiting a significant increase in $PM_{2.5}$ intensity generally aligned with the regions with significant increases in HPE duration (Figure 1c), except for some high $PM_{2.5}$ intensity regions at higher latitudes in the Northern Hemisphere (Figure 1e). This association indicates that people in these regions experienced more intense HPEs (prolonged duration and higher maximum $PM_{2.5}$ concentration level). A significant linear increase in HPE $PM_{2.5}$ intensity occurred in continental Southeast Asia (Figure 1e), with a rate of around 6.8 μg m^{-3} $year^{-1}$. Figure 1f presents the zonal mean differences between the most recent decade and the first decade, which aggregates all the grids along each latitude and better captures abruptly increased wildfire activities in the recent decade (Figure 2c). The zonal-mean profile emphasized the severity in and around subtropical regions in the Northern Hemisphere (Figure 1f). However, the $PM_{2.5}$ intensity peak occurred around 60° latitude in the Northern Hemisphere, with an average concentration in the recent decade higher than 200 μg m^{-3} (Figure 1f), even though only a few significant linear increases were revealed in regions at this latitude such as the US and Russia (Figure 1e). From a zonal mean perspective, the pattern of increasing temperature intensity was comparable to that of $PM_{2.5}$ during HPEs (Figure 1g), with a linear trend of approximately 0.01°C per year globally. This indicates that regions with increasing extreme pollution levels during HPEs were simultaneously experiencing an increase in extreme temperature. For subtropical regions of the Northern Hemisphere, the $PM_{2.5}$ intensity reached approximately 150 μg m^{-3} (Figure 1f) together with temperatures higher than 40°C (Figure 1h). In a nutshell, the HPE frequency increased significantly globally, while the significant increases in duration and intensity (in terms of both $PM_{2.5}$ and temperature) were more centralized in tropical and subtropical regions in both Hemispheres. Transboundary air pollution or biomass burning activities played essential roles in such HPE increases in those vulnerable regions based on our further composite analysis. Details can be found in Text S1 in Supporting Information S1.

3.2. Inequality in HPE Evolution Between the Global North and the Global South

We further calculated the HPE variations in both the Global North and the Global South (see methods) to illustrate the regional difference and environmental inequality (Figure 2). HPE frequency in the Global North (7.4 days $year^{-1}$) was significantly ($p < 0.001$ in t-test) higher than that in the Global South (5.2 days $year^{-1}$), with comparable linear increasing trends (Figure 2a). Oppositely, temperature intensity in the Global South was significantly higher than in the Global North (Figure 2d), which could be attributed to the fact that many of the Global South countries are in subtropical and tropical areas. No significant difference was found in HPE duration between the Global North and the Global South (Figure 2b), even though the Global South showed a faster increase in duration than the Global North.

Before 2010, the HPE $PM_{2.5}$ intensity in the Global North (58.1 μg m^{-3}) remained relatively low compared to the Global South (93.5 μg m^{-3}). However, after 2010, the $PM_{2.5}$ intensity in the Global North increased significantly, becoming 33.3% higher than in the Global South, with an annual increase of 4.1 μg m^{-3}. In contrast, the increase in the Global South was marginal (Figure 2c). This reversal can be attributed to a substantial rise in $PM_{2.5}$ concentration in the Western coastal regions of the US, Canada, and the Russian Arctic during 2010–2019 (Figure 2f), compared to the period 1 of 990−2009 (Figure 2e).

3.3. Premature Mortality Associated With $PM_{2.5}$ Exposure in HPEs

To estimate the global burden of premature mortality during HPEs, we first derived a concentration–response function (CRF) for acute $PM_{2.5}$ exposure during HPEs, and applied the CRF to estimate the resultant $PM_{2.5}$-associated excess premature mortality on HPE days during the past three decades in each country. Our finding shows that an increase of 10 μg per cubic meter of $PM_{2.5}$ concentration was associated with a 0.66% increase [95% confidence interval (CI): 0.53%–0.85%] in the relative risk of $PM_{2.5}$-associated premature mortality (all-cause, all-age) during HPEs on a global scale (Figure 3a).

We estimated approximately 23,103 (95% CI: 22,405−24,371) premature mortalities due to $PM_{2.5}$ exposure occurred every year globally during HPEs, with a significant increasing trend of 874 premature mortalities per year (Figure S6 in Supporting Information S1). The highest annual premature mortality of 39,047 (95% CI: 37,966−41,587) occurred recently in 2010 (Figure S6 in Supporting Information S1). The significant increasing trend (839 premature mortalities per year) in the Global South contributed to 96% of the global increase trend, while the mortality changes in the Global North were not significant (35 mortalities per year with $p = 0.19$, Figure 3b). Although the increase in HPEs in the Global North was significant in the context of climate change

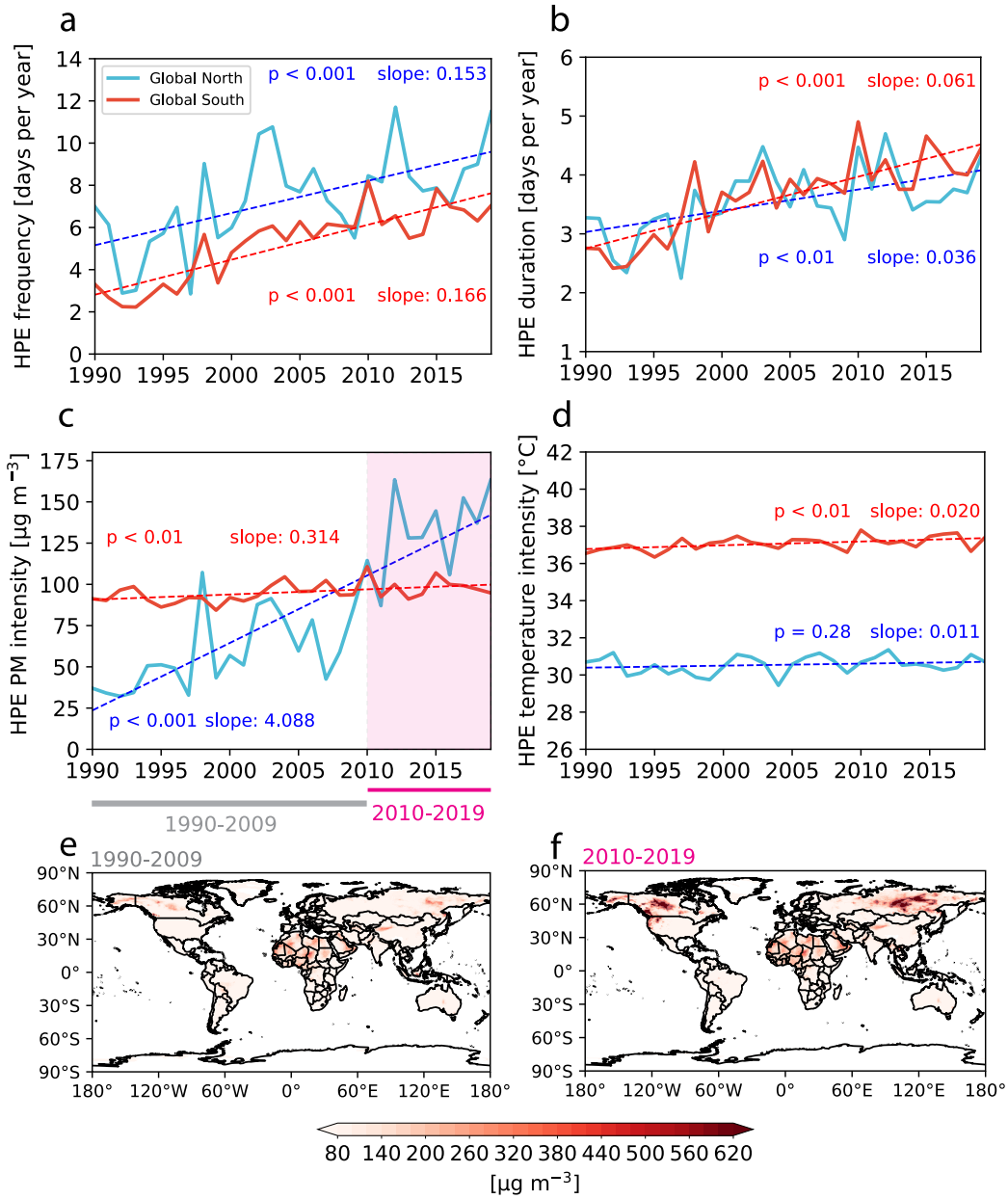

Figure 2. Spatial differences in HPEs between the Global North and the Global South. (a) Time series of HPE frequency changes from 1990 to 2019. (b) Time series of HPE duration changes from 1990 to 2019. (c) Time series of HPE $PM_{2.5}$ intensity changes from 1990 to 2019. Magenta shading stands for the period (2010–2019) with continuously higher $PM_{2.5}$ intensity in the Global North than in the Global South. (d) Time series of HPE temperature intensity changes from 1990 to 2019. (e) Mean HPE $PM_{2.5}$ intensity averaged from 1990 to 2009. (f) Mean HPE $PM_{2.5}$ intensity averaged from 2010 to 2019. The slope and the corresponding *p*-value in each linear regression fitting are shown for both the Global North and the Global South.

over the past 30 years (Figure 2), the relatively lower number of mortalities and insignificant changes indicate an overall better social well-being and resilience in the Global North countries. In contrast, the increasing population and more severe living conditions in the Global South countries have subjected their populations to a substantial burden of deaths during HPEs.

We found a remarkable inequality between the Global North and the Global South regarding the 30-year total premature mortality attributable to $PM_{2.5}$ exposure during HPEs. The number of 30-year premature mortalities in the Global South was estimated 560,875 (95% CI: 555,701−578,200), accounting for approximately 80% of the

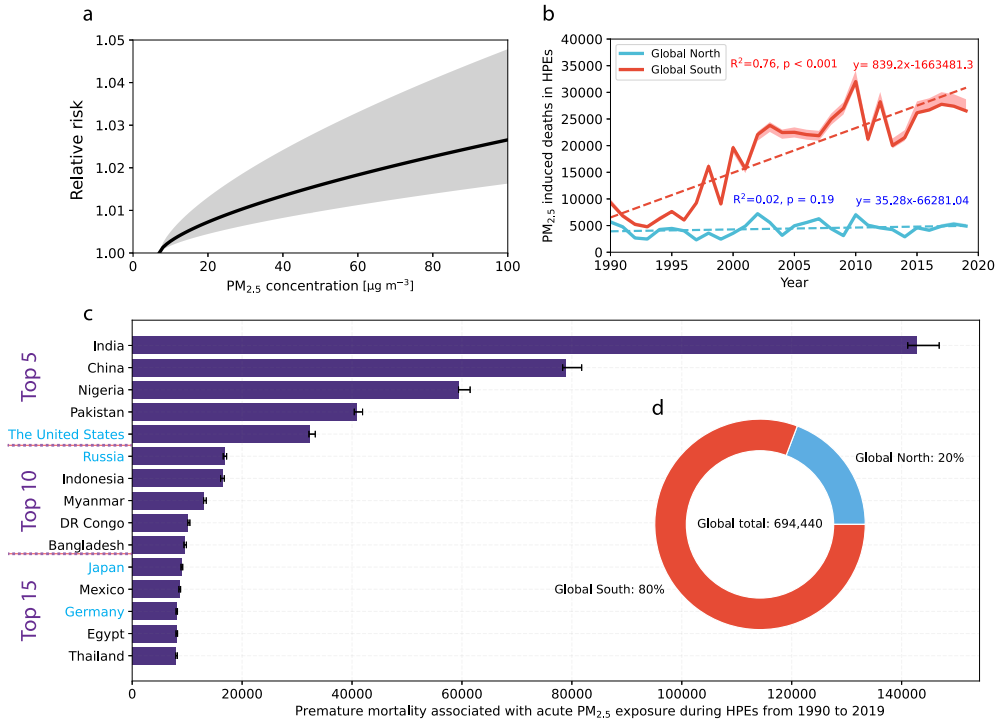

Figure 3. Global burden of premature mortality associated with acute $PM_{2.5}$ exposure during HPEs. (a) Concentration-Response function for premature mortality associated with $PM_{2.5}$ exposure during HPEs. The gray shading indicates the 95% confidence interval (CI). (b) Annual changes in premature mortality associated with exposure to $PM_{2.5}$ during HPEs from 1990 to 2019. The shading indicates the 95% CI. (c) Top 15 countries for premature mortality associated with exposure to $PM_{2.5}$ during HPEs from 1990 to 2019. (d) Pie chart of premature mortality associated with exposure to $PM_{2.5}$ during HPEs in the Global North and the Global South from 1990 to 2019. The 95% CI numbers are not shown. The black error bars in (c) indicate the 95% CI. The Global North countries in (c) are highlighted in blue.

overall global premature mortalities [694,440 (95% CI: 687,996−715,311)] (Figure 3d) and being 3 times higher than those occurred in the Global North [133,565 (95% CI: 132,295−137,111)].

At the country level, the United States was the most vulnerable Global North country on the Top 15 list with the highest mortality burden of 32,227 (95% CI: 32,163−33,313) during HPEs, followed by Russia, Japan, and Germany (Figure 3c). Our estimates show approximately 142,765 people (95% CI: 141,108−146,831) died in India during HPEs from 1990 to 2019 due to exposure to $PM_{2.5}$, marking the highest number of premature mortality across the world (Figure 3c). The burden in India surpassed the combined burdens of the second-and third-ranking countries, namely, China and Nigeria, respectively. Most countries with prominent burdens are from the Global South and are within the vulnerable regions (Figure S7 in Supporting Information S1) identified. These results indicate the remarkable inequality in the mortality burden of HPEs.

4. Discussion

The compound increase in $PM_{2.5}$ and temperature intensity could elevate the risk of fatality if people are exposed to this hot-and-polluted environment even for only a few days (R. Xu et al., 2023). This study found that the relative risk of $PM_{2.5}$-associated premature mortality during HPEs was higher than during regular days. We estimated a 0.66% (95% CI: 0.53%–0.85%) increase in the relative risk of $PM_{2.5}$-associated premature mortality (all-cause, all-age) for every increase of 10 μg per cubic meter of $PM_{2.5}$ concentration during HPEs on a global scale. A global review study estimated a relative risk increase of 0.65% (95% CI: 0.44%–0.86%) by meta-analysis (Orellano et al., 2020). In this study, we revealed a slightly higher relative risk when taking the hot environment into account, pinpointing the potential synergistic health effect of $PM_{2.5}$ exposure during HPEs. Meanwhile, insufficient studies provide us with precise premature mortality estimates considering mortalities associated with heat during HPEs, making our study most likely to underestimate the overall burden of HPEs. This also implies

that the overall health burden might be even higher, indicating the urgency to protect global population health from HPEs.

Our findings clearly pointed out the inequality in the health burdens due to $PM_{2.5}$ exposure during HPEs between the Global South and the Global North during the past three decades. We identified India as the most vulnerable country globally to the public health threats posed by HPEs. The alarming situation faced by India has attracted widespread attention in recent years. Precisely controlling specific air pollutants, especially ammonia, elemental carbon, and organic carbon, is critical for India because these components have been reported to have a greater impact on premature mortality than the total $PM_{2.5}$ mass concentration in India (Joshi et al., 2022). The adverse effects of these air pollutants will be magnified along with the rapid increase in HPEs revealed in this study. Reducing the population exposure time during HPEs can effectively avoid excessive risk (Sorensen & Hess, 2022). Very few policies, including warning systems, have been implemented in the Global South countries to safeguard outdoor workers during heatwaves and air pollution, even though the Global South countries are more susceptible to HPEs. Adequate cooling facilities and heat-related policies, such as more frequent and longer mandatory rest times, are urgently needed to support vulnerable groups and outdoor workers in the Global South countries under climate change, where energy accessibility remains one of the biggest challenges nowadays (Sherman et al., 2022). In addition, more stringent and health-orientated air pollutant emission control policies are required to reduce the occurrence of air pollution episodes and, thus, human health burdens in the Global South countries (T. Fang et al., 2023; Gu & Yim, 2016; Yim et al., 2024). Furthermore, the anticipated increase in HPE incidence in the future may pose challenges related to the massive demand for electricity in these economically challenged countries. This factor must be considered in future power system planning to ensure sustainable and resilient energy infrastructure in the Global South (Sherman et al., 2022).

Mitigation of air pollution and climate change should be implemented simultaneously to achieve co-benefits (Gómez-Sanabria et al., 2022). We found the contributions of wildfires to the increase in HPE $PM_{2.5}$ intensity in the Global North countries such as the US, Canada, and Russia after 2010. For example, a recent study by Wei, Wang, et al. (2023) reported a rise in wildfire-attributable $PM_{2.5}$ concentrations in the US after 2010, suggesting that wildfires could be the leading cause of air quality deterioration, offsetting the efforts from emission controls in the Global North. These findings imply that the Global North may face a renewed risk of air pollution in a global warming environment despite several years of emission control measures. Wildfires are a typical source of HPEs because they can simultaneously generate massive amounts of heat and air pollutants (R. Xu et al., 2020). In a single year of 2020, 16.5 million people were impacted during the California wildfire events by such synergistic effects (Rosenthal et al., 2022). Moreover, wildfires are highly susceptible to the influences of climate change (X. Huang et al., 2023) and climate variability, that is, ENSO (Yim et al., 2024), that may induce hot and dry climate conditions favorable for wildfires. Other observations have revealed a trend of increasing wildfires in recent years, for example, wildfires in the western United States in 2018 and 2020 (R. Xu et al., 2020). The radiative forcing by aerosols (Myhre et al., 2013; Samset et al., 2013; Schulz et al., 2006) generated by wildfires further contributes to modifying near-surface atmospheric conditions, exacerbating drought conditions, and fostering the occurrence of more fires (X. Huang et al., 2023). This wildfire smoke–weather interaction should also be considered for HPE mitigation. This highlights the importance of addressing climate change and air quality simultaneously to achieve co-benefits for human health when implementing environmental policies.

The uncertainties in this study primarily arose from the estimation of parameters in the CRF, that is, utilizing meta-analysis. Given the limited number of studies that have investigated the relative health risk of $PM_{2.5}$ exposure coupled with hot environments, employing meta-analysis currently remains the most practical approach for obtaining a global estimation. Despite our strict selection of studies conducted under high-temperature conditions, isolating the impact of high temperature on pollution-related mortality remains challenging because pollutant concentrations can still correlate with temperature variations. This interdependency highlights the need for further research using advanced modeling techniques to distinguish the direct effects of high temperature from those of $PM_{2.5}$ exposure. To account for additional uncertainties arising from $PM_{2.5}$ data sets, population interpolation, and the CRF equation, we employed the Monte Carlo method to calculate the 95% CIs for the results. Our collected data sets from the literature (Table S1 in Supporting Information S1) had insufficient data from Africa, India, and Southeast Asia, where the burden of premature mortality was significantly high (Figure 3c). This data gap may lead to an underestimation of the global health burden of HPEs. In other words, this finding implies that the actual health burden could be more severe than our estimation. These limitations emphasize the need for further research and data collection in regions with substantial health risks associated with

$PM_{2.5}$ exposure in hot environments. Overall, our study provides a reasonable global estimate of $PM_{2.5}$-associated mortality burden during HPEs, which is a reliable reference for implementing mitigation strategies in the future to reduce its adverse health effects on human health.

5. Conclusions

This study comprehensively analyzed the global spatiotemporal characteristics of HPEs from 1990 to 2019 and estimated the global premature mortality associated with acute $PM_{2.5}$ exposure during HPEs. We found that HPE frequency increased significantly globally, while the significant increases in duration and intensity (in terms of both $PM_{2.5}$ and temperature) were more centralized in tropical and subtropical regions in both hemispheres. HPE $PM_{2.5}$ intensity in the Global North continuously rose, overpassing the Global South after 2010, implying a returned risk of air pollution in the context of climate change in the Global North after several years of emission control endeavors. However, the Global South dominated the premature mortality estimated based on the CRF derived for acute $PM_{2.5}$ exposure during HPEs, occupying approximately 80% of the total mortality globally. Among the Top 15 countries, India had by far the highest number of HPE-attributable premature mortality, whereas the United States, Russia, Japan, and Germany were particularly highlighted as the most vulnerable countries in the Global North, pinpointing the importance of considering environmental inequality during policymaking processes.

Conflict of Interest

The authors declare no conflicts of interest relevant to this study.

Data Availability Statement

Data is available at Copernicus Climate Change Service (2020), Hersbach et al. (2023), Global Modeling and Assimilation Office (GMAO) (2015), Institute for Health Metrics and Evaluation (IHME) (2024), WorldPop (2018), Schiavina et al. (2023), and World Population Review (2025).

Acknowledgments
This research is jointly supported by the Ministry of Education, Singapore, under its MOE AcRF Tier 3 Award MOET32022-0006, the Start-up Grant (021452-00001) (LKC) and Start-up Grant (021384-00001) for Assoc. Prof. Yim (ASE), the MOE Academic Research Fund (AcRF) Tier 1 Project (022713-00001) and EOS FY2022 funding (award no: EOS MOE RCE FY 2022).

References

Anenberg, S. C., Haines, S., Wang, E., Nassikas, N., & Kinney, P. L. (2020). Synergistic health effects of air pollution, temperature, and pollen exposure: A systematic review of epidemiological evidence. *Environmental Health*, *19*(1), 130. https://doi.org/10.1186/s12940-020-00681-z

Atkinson, R. W., Kang, S., Anderson, H. R., Mills, I. C., & Walton, H. A. (2014). Epidemiological time series studies of $PM_{2.5}$ and daily mortality and hospital admissions: A systematic review and meta-analysis. *Thorax*, *69*(7), 660–665. https://doi.org/10.1136/thoraxjnl-2013-204492

Borchers Arriagada, N., Bowman, D. M. J. S., Palmer, A. J., & Johnston, F. H. (2020). Climate change, wildfires, heatwaves and health impacts in Australia. In R. Akhtar (Ed.), *Extreme weather events and human health: International case studies* (pp. 99–116). Springer International Publishing. https://doi.org/10.1007/978-3-030-23773-8_8

Buchard, V., da Silva, A. M., Randles, C. A., Colarco, P., Ferrare, R., Hair, J., et al. (2016). Evaluation of the surface $PM_{2.5}$ in Version 1 of the NASA MERRA aerosol reanalysis over the United States. *Atmospheric Environment*, *125*, 100–111. https://doi.org/10.1016/j.atmosenv.2015.11.004

Buchard, V., Randles, C. A., da Silva, A. M., Darmenov, A., Colarco, P. R., Govindaraju, R., et al. (2017). The MERRA-2 aerosol reanalysis, 1980 onward. Part II: Evaluation and case studies. *Journal of Climate*, *30*(17), 6851–6872. https://doi.org/10.1175/JCLI-D-16-0613.1

Campbell, S., Remenyi, T. A., White, C. J., & Johnston, F. H. (2018). Heatwave and health impact research: A global review. *Health and Place*, *53*, 210–218. https://doi.org/10.1016/j.healthplace.2018.08.017

Chambers, J. (2020). Global and cross-country analysis of exposure of vulnerable populations to heatwaves from 1980 to 2018. *Climatic Change*, *163*(1), 539–558. https://doi.org/10.1007/s10584-020-02884-2

Chiu, K.-C., Hsieh, M.-S., Huang, Y.-T., & Liu, C.-Y. (2024). Exposure to ambient temperature and heat index in relation to DNA methylation age: A population-based study in Taiwan. *Environment International*, *186*, 108581. https://doi.org/10.1016/j.envint.2024.108581

Cohen, A. J., Brauer, M., Burnett, R., Anderson, H. R., Frostad, J., Estep, K., et al. (2017). Estimates and 25-year trends of the global burden of disease attributable to ambient air pollution: An analysis of data from the global burden of diseases study 2015. *The Lancet*, *389*(10082), 1907–1918. https://doi.org/10.1016/S0140-6736(17)30505-6

Cohen, J. B., Lecoeur, E., & Hui Loong Ng, D. (2017). Decadal-scale relationship between measurements of aerosols, land-use change, and fire over Southeast Asia. *Atmospheric Chemistry and Physics*, *17*(1), 721–743. https://doi.org/10.5194/acp-17-721-2017

Copernicus Climate Change Service. (2020). Near surface meteorological variables from 1979 to 2018 derived from bias-corrected reanalysis [Dataset]. *ECMWF*. https://doi.org/10.24381/CDS.20D54E34

Cucchi, M., Weedon, G. P., Amici, A., Bellouin, N., Lange, S., Müller Schmied, H., et al. (2020). WFDE5: Bias-adjusted ERA5 reanalysis data for impact studies. *Earth System Science Data*, *12*(3), 2097–2120. https://doi.org/10.5194/essd-12-2097-2020

Curriero, F. C., Heiner, K. S., Samet, J. M., Zeger, S. L., Strug, L., & Patz, J. A. (2002). Temperature and mortality in 11 cities of the Eastern United States. *American Journal of Epidemiology*, *155*(1), 80–87. https://doi.org/10.1093/aje/155.1.80

Deschênes, O., & Greenstone, M. (2011). Climate change, mortality, and adaptation: Evidence from annual fluctuations in weather in the US. *American Economic Journal: Applied Economics*, *3*(4), 152–185. https://doi.org/10.1257/app.3.4.152

Doherty, R. M., Heal, M. R., & O'Connor, F. M. (2017). Climate change impacts on human health over Europe through its effect on air quality. *Environmental Health*, *16*(1), 118. https://doi.org/10.1186/s12940-017-0325-2

Dong, Z., Wang, L., Sun, Y., Hu, T., Limsakul, A., Singhruck, P., & Pimonsree, S. (2021). Heatwaves in Southeast Asia and their changes in a warmer world. *Earth's Future*, *9*(7), e2021EF001992. https://doi.org/10.1029/2021EF001992

Fang, C., Zhu, B., Pan, C., Yun, X., Ding, D., & Tao, S. (2020). Regional and sectoral sources for black carbon over South China in spring and their sensitivity to East Asian summer monsoon onset. *Journal of Geophysical Research: Atmospheres*, *125*(20), e2020JD033219. https://doi.org/10.1029/2020JD033219

Fang, T., Gu, Y., & Yim, S. H. L. (2023). Assessing local and transboundary fine particulate matter pollution and sectoral contributions in Southeast Asia during haze months of 2015–2019. *Science of the Total Environment*, *912*, 169051. https://doi.org/10.1016/j.scitotenv.2023.169051

Global Modeling and Assimilation Office (GMAO). (2015). MERRA-2 tavg1_2d_aer_Nx: 2d,1-Hourly,Time-averaged,Single-Level,Assimilation,Aerosol Diagnostics V5.12.4, Greenbelt, MD, USA [Dataset]. *Goddard Earth Sciences Data and Information Services Center (GES DISC)*. https://doi.org/10.5067/KLICLTZ8EM9D

Gómez-Sanabria, A., Kiesewetter, G., Klimont, Z., Schoepp, W., & Haberl, H. (2022). Potential for future reductions of global GHG and air pollutants from circular waste management systems. *Nature Communications*, *13*(1), 106. https://doi.org/10.1038/s41467-021-27624-7

Gu, Y., & Yim, S. H. L. (2016). The air quality and health impacts of domestic trans-boundary pollution in various regions of China. *Environment International*, *97*, 117–124. https://doi.org/10.1016/j.envint.2016.08.004

Hansen, A., Bi, P., Nitschke, M., Ryan, P., Pisaniello, D., & Tucker, G. (2008). The effect of heat waves on mental health in a temperate Australian City. *Environmental Health Perspectives*, *116*(10), 1369–1375. https://doi.org/10.1289/ehp.11339

Health, T. L. P. (2023). Public health in China: Time to invest in prevention. *The Lancet Public Health*, *8*(12), e905. https://doi.org/10.1016/S2468-2667(23)00278-5

Hersbach, H., Bell, B., Berrisford, P., Biavati, G., Horányi, A., Muñoz Sabater, J., et al. (2023). ERA5 hourly data on pressure levels from 1940 to present [Dataset]. *Copernicus Climate Change Service (C3S) Climate Data Store (CDS)*. https://doi.org/10.24381/cds.bd0915c6

Hong, C., Zhang, Q., Zhang, Y., Davis, S. J., Tong, D., Zheng, Y., et al. (2019). Impacts of climate change on future air quality and human health in China. *Proceedings of the National Academy of Sciences of the United States of America*, *116*(35), 17193–17200. https://doi.org/10.1073/pnas.1812881116

Huang, T., Gu, Y., Lallemant, D., Lau, G. N. C., Sung, J. J. Y., & Yim, S. H. L. (2024). Equatorward shift of the boreal summer intertropical convergence zone in Maritime Continent and the impacts on surface black carbon concentration and public health. *Npj Climate and Atmospheric Science*, *7*(1), 1–8. https://doi.org/10.1038/s41612-024-00593-6

Huang, X., Ding, K., Liu, J., Wang, Z., Tang, R., Xue, L., et al. (2023). Smoke-weather interaction affects extreme wildfires in diverse coastal regions. *Science*, *379*(6631), 457–461. https://doi.org/10.1126/science.add9843

Institute for Health Metrics and Evaluation (IHME). (2024). GBD results [Dataset]. *IHME, University of Washington*. Retrieved from https://vizhub.healthdata.org/gbd-results

Janssen, N. A. H., Fischer, P., Marra, M., Ameling, C., & Cassee, F. R. (2013). Short-term effects of $PM_{2.5}$, PM_{10} and $PM_{2.5-10}$ on daily mortality in The Netherlands. *Science of the Total Environment*, *463–464*, 20–26. https://doi.org/10.1016/j.scitotenv.2013.05.062

Joshi, P., Dey, S., Ghosh, S., Jain, S., & Sharma, S. K. (2022). Association between acute exposure to $PM_{2.5}$ Chemical species and mortality in Megacity Delhi, India. *Environmental Science & Technology*, *56*(11), 7275–7287. https://doi.org/10.1021/acs.est.1c06864

Kinney, P. L., & Pinkerton, K. E. (2022). Heatwaves and air pollution: A deadly combination. *American Journal of Respiratory and Critical Care Medicine*, *206*(9), 1060–1062. https://doi.org/10.1164/rccm.202207-1372ED

Li, D., Yuan, J., & Kopp, R. E. (2020). Escalating global exposure to compound heat-humidity extremes with warming. *Environmental Research Letters*, *15*(6), 064003. https://doi.org/10.1088/1748-9326/ab7d04

Li, T., Guo, Y., Liu, Y., Wang, J., Wang, Q., Sun, Z., et al. (2019). Estimating mortality burden attributable to short-term $PM_{2.5}$ exposure: A national observational study in China. *Environment International*, *125*, 245–251. https://doi.org/10.1016/j.envint.2019.01.073

Li, Y., Hong, T., Gu, Y., Li, Z., Huang, T., Lee, H. F., et al. (2023). Assessing the spatiotemporal characteristics, factor importance, and health impacts of air pollution in Seoul by integrating Machine learning into land-use regression modeling at high spatiotemporal resolutions. *Environmental Science & Technology*, *57*(3), 1225–1236. https://doi.org/10.1021/acs.est.2c03027

Liu, C., Chen, R., Sera, F., Vicedo-Cabrera, A. M., Guo, Y., Tong, S., et al. (2019). Ambient particulate air pollution and daily mortality in 652 cities. *New England Journal of Medicine*, *381*(8), 705–715. https://doi.org/10.1056/NEJMoa1817364

McGeehin, M. A., & Mirabelli, M. (2001). The potential impacts of climate variability and change on temperature-related morbidity and mortality in the United States. *Environmental Health Perspectives*, *109*, 185–189. https://doi.org/10.2307/3435008

McKinnon, K. A., & Simpson, I. R. (2022). How Unexpected was the 2021 Pacific Northwest heatwave? *Geophysical Research Letters*, *49*(18), e2022GL100380. https://doi.org/10.1029/2022GL100380

Moolgavkar, S. H. (2003). Air pollution and daily mortality in two U.S. Counties: Season-specific analyses and exposure-response relationships. *Inhalation Toxicology*, *15*(9), 877–907. https://doi.org/10.1080/08958370390215767

Mukherjee, S., Dasgupta, S., Mishra, P. K., & Chaudhury, K. (2021). Air pollution-induced epigenetic changes: Disease development and a possible link with hypersensitivity pneumonitis. *Environmental Science and Pollution Research International*, *28*(40), 55981–56002. https://doi.org/10.1007/s11356-021-16056-x

Myhre, G., Samset, B. H., Schulz, M., Balkanski, Y., Bauer, S., Berntsen, T. K., et al. (2013). Radiative forcing of the direct aerosol effect from AeroCom Phase II simulations. *Atmospheric Chemistry and Physics*, *13*(4), 1853–1877. https://doi.org/10.5194/acp-13-1853-2013

Nduka, I. C., Huang, T., Li, Z., Yang, Y., & Yim, S. H. L. (2022). Long-term trends of atmospheric hot-and-polluted episodes (HPE) and the public health implications in the Pearl River Delta region of China. *Environmental Pollution*, *311*, 119782. https://doi.org/10.1016/j.envpol.2022.119782

Orellano, P., Reynoso, J., Quaranta, N., Bardach, A., & Ciapponi, A. (2020). Short-term exposure to particulate matter (PM_{10} and $PM_{2.5}$), nitrogen dioxide (NO_2), and ozone (O_3) and all-cause and cause-specific mortality: Systematic review and meta-analysis. *Environment International*, *142*, 105876. https://doi.org/10.1016/j.envint.2020.105876

Parliari, D., Economou, T., Giannaros, C., Kushta, J., Melas, D., Matzarakis, A., & Lelieveld, J. (2024). A comprehensive approach for assessing synergistic impact of air quality and thermal conditions on mortality: The case of Thessaloniki, Greece. *Urban Climate*, *56*, 102088. https://doi.org/10.1016/j.uclim.2024.102088

Pascal, M., Falq, G., Wagner, V., Chatignoux, E., Corso, M., Blanchard, M., et al. (2014). Short-term impacts of particulate matter (PM_{10}, $PM_{10-2.5}$, $PM_{2.5}$) on mortality in nine French cities. *Atmospheric Environment*, *95*, 175–184. https://doi.org/10.1016/j.atmosenv.2014.06.030

Perkins-Kirkpatrick, S. E., & Lewis, S. C. (2020). Increasing trends in regional heatwaves. *Nature Communications*, *11*(1), 3357. https://doi.org/10.1038/s41467-020-16970-7

Pozzer, A., Anenberg, S. C., Dey, S., Haines, A., Lelieveld, J., & Chowdhury, S. (2023). Mortality attributable to ambient air pollution: A review of global estimates. *GeoHealth*, *7*(1), e2022GH000711. https://doi.org/10.1029/2022GH000711

Qian, Y., Hsu, P.-C., Yuan, J., Zhu, Z., Wang, H., & Duan, M. (2022). Effects of subseasonal variation in the East Asian Monsoon system on the summertime heat wave in western North America in 2021. *Geophysical Research Letters*, *49*(8), e2021GL097659. https://doi.org/10.1029/2021GL097659

Rider, C. F., & Carlsten, C. (2019). Air pollution and DNA methylation: Effects of exposure in humans. *Clinical Epigenetics*, *11*(1), 131. https://doi.org/10.1186/s13148-019-0713-2

Rosenthal, N., Benmarhnia, T., Ahmadov, R., James, E., & Marlier, M. E. (2022). Population co-exposure to extreme heat and wildfire smoke pollution in California during 2020. *Environmental Research: Climate*, *1*(2), 025004. https://doi.org/10.1088/2752-5295/ac860e

Sahu, L. K., Kondo, Y., Miyazaki, Y., Pongkiatkul, P., & Kim Oanh, N. T. (2011). Seasonal and diurnal variations of black carbon and organic carbon aerosols in Bangkok. *Journal of Geophysical Research*, *116*(D15), D15302. https://doi.org/10.1029/2010JD015563

Samset, B. H., Myhre, G., Schulz, M., Balkanski, Y., Bauer, S., Berntsen, T. K., et al. (2013). Black carbon vertical profiles strongly affect its radiative forcing uncertainty. *Atmospheric Chemistry and Physics*, *13*(5), 2423–2434. https://doi.org/10.5194/acp-13-2423-2013

Schiavina, M., Freire, S., Carioli, A., & MacManus, K. (2023). GHS-POP R2023A—GHS Population Grid Multitemporal. (1975–2030) [Dataset]. *European commission, Joint Research Centre (JRC)*. https://doi.org/10.2905/2FF68A52-5B5B-4A22-8F40-C41DA8332CFE

Schulz, M., Textor, C., Kinne, S., Balkanski, Y., Bauer, S., Berntsen, T., et al. (2006). Radiative forcing by aerosols as derived from the AeroCom present-day and pre-industrial simulations. *Atmospheric Chemistry and Physics*, *6*(12), 5225–5246. https://doi.org/10.5194/acp-6-5225-2006

Sherman, P., Lin, H., & McElroy, M. (2022). Projected global demand for air conditioning associated with extreme heat and implications for electricity grids in poorer countries. *Energy and Buildings*, *268*, 112198. https://doi.org/10.1016/j.enbuild.2022.112198

Sorensen, C., & Hess, J. (2022). Treatment and prevention of heat-related illness. *New England Journal of Medicine*, *387*(15), 1404–1413. https://doi.org/10.1056/NEJMcp2210623

Thompson, R., Lawrance, E. L., Roberts, L. F., Grailey, K., Ashrafian, H., Maheswaran, H., et al. (2023). Ambient temperature and mental health: A systematic review and meta-analysis. *The Lancet Planetary Health*, *7*(7), e580–e589. https://doi.org/10.1016/S2542-5196(23)00104-3

Underwood, E. (2017). The polluted brain. *Science*, *355*(6323), 342–345. https://doi.org/10.1126/science.355.6323.342

Vanos, J. K., Cakmak, S., Kalkstein, L. S., & Yagouti, A. (2015). Association of weather and air pollution interactions on daily mortality in 12 Canadian cities. *Air Quality, Atmosphere and Health*, *8*(3), 307–320. https://doi.org/10.1007/s11869-014-0266-7

Wei, J., Li, Z., Lyapustin, A., Wang, J., Dubovik, O., Schwartz, J., et al. (2023). First close insight into global daily gapless 1 km $PM_{2.5}$ pollution, variability, and health impact. *Nature Communications*, *14*(1), 8349. https://doi.org/10.1038/s41467-023-43862-3

Wei, J., Wang, J., Li, Z., Kondragunta, S., Anenberg, S., Wang, Y., et al. (2023). Long-term mortality burden trends attributed to black carbon and $PM_{2.5}$ from wildfire emissions across the continental USA from 2000 to 2020: A deep learning modelling study. *The Lancet Planetary Health*, *7*(12), e963–e975. https://doi.org/10.1016/S2542-5196(23)00235-8

WHO global air quality guidelines: particulate matter (PM2.5 and PM10), ozone, nitrogen dioxide, sulfur dioxide and carbon monoxide. (2021). Retrieved from https://www.who.int/publications-detail-redirect/9789240034228

World Population Review. (2025). World population review [Dataset]. Retrieved from https://worldpopulationreview.com

WorldPop (www.worldpop.org—School of Geography and Environmental Science, University of Southampton; Department of Geography and Geosciences, University of Louisville; Departement de Geographie, Universite de Namur) and Center for International Earth Science Information Network (CIESIN), Columbia University. (2018). Global high resolution population denominators project—Funded by The Bill and Melinda Gates Foundation (OPP1134076) [Dataset]. https://doi.org/10.5258/SOTON/WP00645

Xiao, Q., Geng, G., Xue, T., Liu, S., Cai, C., He, K., & Zhang, Q. (2022). Tracking $PM_{2.5}$ and O_3 pollution and the related health burden in China 2013–2020. *Environmental Science & Technology*, *56*(11), 6922–6932. https://doi.org/10.1021/acs.est.1c04548

Xu, R., Huang, S., Shi, C., Wang, R., Liu, T., Li, Y., et al. (2023). Extreme temperature events, fine particulate matter, and myocardial infarction mortality. *Circulation*, *148*(4), 312–323. https://doi.org/10.1161/CIRCULATIONAHA.122.063504

Xu, R., Yu, P., Abramson, M. J., Johnston, F. H., Samet, J. M., Bell, M. L., et al. (2020). Wildfires, global climate change, and human health. *New England Journal of Medicine*, *383*(22), 2173–2181. https://doi.org/10.1056/NEJMsr2028985

Xu, Y., Tian, C., Ma, J., Wang, X., Li, J., Tang, J., et al. (2013). Assessing cancer risk in China from γ-hexachlorocyclohexane emitted from Chinese and Indian sources. *Environmental Science & Technology*, *47*(13), 7242–7249. https://doi.org/10.1021/es400141e

Xu, Y., Wu, X., Kumar, R., Barth, M., Diao, C., Gao, M., et al. (2020). Substantial increase in the joint occurrence and human exposure of heatwave and high-PM hazards over South Asia in the Mid-21st century. *AGU Advances*, *1*(2), e2019AV000103. https://doi.org/10.1029/2019AV000103

Yim, S. H. L. (2020). Development of a 3D real-time atmospheric monitoring system (3DREAMS) using doppler LiDARs and applications for long-term analysis and hot-and-polluted episodes. *Remote Sensing*, *12*(6), 1036. https://doi.org/10.3390/rs12061036

Yim, S. H. L., Hou, X., Guo, J., & Yang, Y. (2019). Contribution of local emissions and transboundary air pollution to air quality in Hong Kong during El Niño-Southern Oscillation and heatwaves. *Atmospheric Research*, *218*, 50–58. https://doi.org/10.1016/j.atmosres.2018.10.021

Yim, S. H. L., Li, Y., Huang, T., Lim, J. T., Lee, H. F., Chotirmall, S. H., et al. (2024). Global health impacts of ambient fine particulate pollution associated with climate variability. *Environment International*, *186*, 108587. https://doi.org/10.1016/j.envint.2024.108587

Zhang, Y., Tao, S., Shen, H., & Ma, J. (2009). Inhalation exposure to ambient polycyclic aromatic hydrocarbons and lung cancer risk of Chinese population. *Proceedings of the National Academy of Sciences of the United States of America*, *106*(50), 21063–21067. https://doi.org/10.1073/pnas.0905756106

Zong, L., Yang, Y., Xia, H., Gao, M., Sun, Z., Zheng, Z., et al. (2022). Joint occurrence of heatwaves and ozone pollution and increased health risks in Beijing, China: Role of synoptic weather pattern and urbanization. *Atmospheric Chemistry and Physics*, *22*(10), 6523–6538. https://doi.org/10.5194/acp-22-6523-2022

References From the Supporting Information

Burke, M., Childs, M. L., de la Cuesta, B., Qiu, M., Li, J., Gould, C. F., et al. (2023). The contribution of wildfire to $PM_{2.5}$ trends in the USA. *Nature*, *622*(7984), 1–6. https://doi.org/10.1038/s41586-023-06522-6

Cochrane, M. A., & Barber, C. P. (2009). Climate change, human land use and future fires in the Amazon. *Global Change Biology*, *15*(3), 601–612. https://doi.org/10.1111/j.1365-2486.2008.01786.x

Dumka, U. C., Kaskaoutis, D. G., Francis, D., Chaboureau, J.-P., Rashki, A., Tiwari, S., et al. (2019). The role of the intertropical discontinuity region and the heat low in dust emission and transport over the Thar Desert, India: A Premonsoon case study. *Journal of Geophysical Research: Atmospheres*, *124*(23), 13197–13219. https://doi.org/10.1029/2019JD030836

Fonseca, M. G., Alves, L. M., Aguiar, A. P. D., Arai, E., Anderson, L. O., Rosan, T. M., et al. (2019). Effects of climate and land-use change scenarios on fire probability during the 21st century in the Brazilian Amazon. *Global Change Biology*, *25*(9), 2931–2946. https://doi.org/10.1111/gcb.14709

Jiang, H., Farrar, J. T., Beardsley, R. C., Chen, R., & Chen, C. (2009). Zonal surface wind jets across the Red Sea due to mountain gap forcing along both sides of the Red Sea. *Geophysical Research Letters*, *36*(19). https://doi.org/10.1029/2009GL040008

Kalenderski, S., & Stenchikov, G. (2016). High-resolution regional modeling of summertime transport and impact of African dust over the Red Sea and Arabian Peninsula. *Journal of Geophysical Research: Atmospheres*, *121*(11), 6435–6458. https://doi.org/10.1002/2015JD024480

Le Page, Y., Morton, D., Hartin, C., Bond-Lamberty, B., Pereira, J. M. C., Hurtt, G., & Asrar, G. (2017). Synergy between land use and climate change increases future fire risk in Amazon forests. *Earth System Dynamics*, *8*(4), 1237–1246. https://doi.org/10.5194/esd-8-1237-2017

Wang, X.-T., Liu, H., Lv, Z.-F., Deng, F.-Y., Xu, H.-L., Qi, L.-J., et al. (2021). Trade-linked shipping CO_2 emissions. *Nature Climate Change*, *11*(11), 945–951. https://doi.org/10.1038/s41558-021-01176-6

Yim, S. H. L., Huang, T., Ho, J. M. W., Lam, A. S. M., Yau, S. T. Y., Yuen, T. W. H., et al. (2022). Rise and fall of lung cancers in relation to tobacco smoking and air pollution: A global trend analysis from 1990 to 2012. *Atmospheric Environment*, *269*, 118835. https://doi.org/10.1016/j.atmosenv.2021.118835

Yin, S. (2020). Biomass burning spatiotemporal variations over South and Southeast Asia. *Environment International*, *145*, 106153. https://doi.org/10.1016/j.envint.2020.106153

Zhou, S., Guo, F., Chao, C.-Y., Yoon, S., Alvarez, S. L., Shrestha, S., et al. (2023). Marine Submicron aerosols from the Gulf of Mexico: Polluted and Acidic with rapid production of Sulfate and Organosulfates. *Environmental Science & Technology*, *57*(13), 5149–5159. https://doi.org/10.1021/acs.est.2c05469